JOURNAL OF SOLID STATE CHEMISTRY 62, 328–334 (1986)

The Structure and Electronic Properties of the Solid Solutions $(Zr_xTi_{1-x})_{1+y}S_2$

DAVID T. HODUL

Varian Research Laboratory, 611 Hansen Way, Palo Alto, California 94303

AND ANGELICA M. STACY[1]

Department of Chemistry, University of California, Berkeley, California 94720

Received May 13, 1985; in revised form September 23, 1985

The solid solutions $(Zr_xTi_{1-x})_{1+y}S_2$ have been prepared and characterized for the full compositional range from ZrS_2 to TiS_2, with $y \simeq 0$. An anomaly in the lattice parameters as a function of composition is observed at $x = 0.5$. For $x < 0.5$, the reaction mixture contains two phases, nonstoichiometric $M_{1+y}S_2$ and a small amount MS_3, but for $x > 0.5$ only stoichiometric MS_2 is formed. X-Ray photoelectron spectra and conductivity measurements show that a metal-to-insulator transition occurs as a function of composition near the anomaly in the lattice parameters at $x = 0.5$. From a calculation based on the cation-to-anion radius ratio, a metal-to-insulator transition is expected to occur near $x = 0$. The discrepancy between this prediction and the observed value of $x = 0.5$ is discussed, as well as the role of nonstoichiometry and disorder in this behavior.

Introduction

The layered transition metal dichalcogenides exhibit a variety of electrical properties from semiconducting ZrS_2 to metallic $Ti_{1+y}S_2$ (*1*). The electronic properties of these binary phases can be manipulated systematically by introducing substitutional dopants (*1, 2*). We have prepared and characterized the solid solutions $(Zr_xTi_{1-x})_{1+y}S_2$ in order to study the electronic properties of these materials and to determine the composition at which a metal–insulator transition occurs. The experiments described below are part of a series (*3–6*) designed to probe the effects of nonstoichiometry, disorder, and structure on the bonding and electronic properties of the layered dichalcogenides.

The IVB transition metal dichalcogenides are prepared by high-temperature reactions (*1, 2*). These materials all have the CdI_2 structure which consists of a hexagonal plane of metal atoms sandwiched between two hexagonal planes of chalcogen atoms. These chalcogen–metal–chalcogen sandwiches are held together by weak van der Waals interactions. The transition metal is coordinated to six chalcogen anions and has a D_{3d} point group symmetry. Although ZrS_2 is found to have a stoichiometry near the ideal chalcogen-to-metal ratio of 2, it is difficult to prepare ordered stoichiometric TiS_2 (*7*). The excess titanium atoms in $Ti_{1+y}S_2$ occupy octrahedral sites in the van der Waals gap.

[1] To whom correspondence should be addressed.

0022-4596/86 $3.00

While ZrS_2 is a semiconductor with a band gap $E_g \sim 1.7$ eV (*1*), debate persists about the electronic structure of $Ti_{1+y}S_2$ (*7*). The band structure calculations of Zunger and Freeman (*8*) and others (*9, 10*) suggest that ordered stoichiometric TiS_2 is also a semiconductor. The metallic conductivity of $Ti_{1+y}S_2$ arises from donor states due to the interstitial titanium atoms; the extra titanium atoms between the layers donate electrons to the empty conduction band of the host material.

Since ZrS_2 is a semiconductor and $Ti_{1+y}S_2$ is a metal due to nonstoichiometry, a metal–insulator transition must occur in the solid solutions $(Zr_xTi_{1-x})_{1+y}S_2$ as a function of composition (*11, 12*). Furthermore, since ZrS_2 is stoichiometric and $Ti_{1+y}S_2$ is nonstoichiometric, a change in stoichiometry is expected to occur also. While several authors have studied the analogous $Hf_xTi_{1-x}S_2$ (*13, 14*) and $Hf_xTi_{1-x}Se_2$ (*15*) systems, no structural anomalies as a function of composition were detected. For the $(Zr_xTi_{1-x})_{1+y}S_2$ phases presented here, a volume anomaly is observed near $x = 0.5$.

The relationship between the metal–insulator transition and the volume anomaly for these materials is discussed below. Resistance measurements as a function of temperature show that a metal–insulator transition occurs for $0.375 < x < 0.500$, near the volume anomaly. Simple models which describe the changes in the energy levels as a

TABLE I

HEXAGONAL LATTICE PARAMETERS

x	a parameter (Å)	c parameter (Å)	Mineralizer	Quality of diffraction pattern	Method of lattice parameter determination	Comments
0.000	3.4055(5)	5.7008(4)	I_2	Excellent	Fit	*a, b, d, f*
0.133	—	—	None	Poor	—	*d, f*
0.150	3.4405(4)	5.7133(6)	I_2	Good	Fit	*d*
0.250	—	—	None	Poor	—	*c, d, e*
0.250	3.4563(10)	5.7220(4)	I_2	Excellent	Fit	*d*
0.250	3.4637(8)	5.7263(9)	I_2	Good	Fit	*d*
0.250	3.4620(14)	5.7228(15)	I_2	Good	Fit	*d*
0.350	—	—	I_2	Poor	—	*d*
0.372	3.501(3)	5.74(5)	None	Poor	Avg	*c, d*
0.497	3.545(5)	5.774(5)	None	Poor	Avg	*c, d*
0.500	3.536(5)	5.758	I_2	Poor	Avg	*a, d*
0.500	3.543(5)	5.772(5)	$TeCl_4$	Poor	Avg	*d*
0.615	3.5756(32)	5.7871(33)	$TeCl_4$	Good	Fit	
0.621	—	—	None	—	—	*c*
0.750	—	—	None	Poor	—	*c*
0.750	3.6016(15)	5.7989(20)	I_2	Good	Fit	
0.750	3.6006(14)	5.7966(4)	$TeCl_4$	Excellent	Fit	
0.875			$TeCl_4$	Excellent	Fit	
1.000	3.6623(8)	5.8258(10)	I_2	Excellent	Fit	*a, b, d, g*

[a] Used for PAS measurements.
[b] Used for ESCA XPS measurements.
[c] Used for conductivity measurements.
[d] Reaction tube contained MX_3 phase.
[e] Lattice parameters are similar to sample with $a = 3.4637$ Å.
[f] Gold color.
[g] Reddish black color.

function of composition suggest that the metal–insulator transition should occur near $x = 0$. The discrepancy between this prediction and the observed value of $x \sim 0.5$ for the transition is discussed, as well as the role of nonstoichiometry and disorder in this behavior. Powder X-ray diffraction data, resistivity measurements, and X-ray photoelectron spectra for these samples are presented.

Experimental

Samples of $(Zr_xTi_{1-x})_{1+y}S_2$ with $0 \leq x \leq 1$ and $y \simeq 0$ were prepared from 99.9% zirconium powder, 99.9% titanium powder, and 99.9999% sulfur lumps (all purchased from Alfa Corp.). The elements were loaded into quartz tubes which had been cleaned by rinsing with dilute hydrofluoric acid and outgassing under a 10^{-5} Torr vacuum. About 5 mg/cm^3 of iodine or $TeCl_4$ was added to some reaction tubes as mineralizing agents to improve the crystallinity of the product (see Table I). The reaction tubes were evacuated to 10^{-5} Torr and sealed. The samples were heated at 600°C for 1 week and then allowed to react at 800°C for 2 to 4 weeks. Samples were cooled to room temperature in approximately 5 min. All products were handled in an inert atmosphere with the oxygen content below 1 ppm and the water content below 10 ppm.

The hexagonal lattice constants were obtained by powder X-ray diffraction analysis using Debye–Scherrer cameras with a diameter of 114.6 mm. Samples were sifted through a ~325-mesh sieve, loaded into 0.3-mm capillaries, and sealed. The diffraction lines were measured to 0.03 mm and distances and angles were determined by the Straumanis method (*16*) which corrects for film shrinkage and systematic errors derived from the camera geometry. Lattice parameters were determined by one of two methods: (a) the "fit" method which used Cohen's least-squares method for hexagonal systems (*17*) using back reflection lines with $\theta > 60°$ and (b) the "avg" method which simply averaged the d spacings observed for the $hk0$ lines for the a parameter and the (001) lines for the c parameter. The avg method was used for samples near the middle of the series as indicated in Table I. The back reflection lines for these samples were so broad that their positions could not be determined accurately and therefore the fit method could not be used. In general, the fit method gave lattice parameters with errors less than 0.001 Å while the precision of the avg method was 0.005 Å.

X-Ray photoelectron spectra were taken for the samples of nominal composition TiS_2, ZrS_2, and $Zr_{0.5}Ti_{0.5}S_2$ mineralized with iodine. Pellets were pressed in air and loaded into a McPherson ESCA 36 photoelectron spectrometer. The samples were exposed to air for approximately 1 min. The incident photons were generated by a magnesium X-ray source and the sample chamber vacuum was about 10^{-9} Torr. Charging of the sample was a problem for the sample of ZrS_2 but not for the samples of nominal composition $Zr_{0.5}Ti_{0.5}S_2$ and TiS_2. All XPS energies were corrected for shifts resulting from charging by calibrations against the XPS energies of carbon peaks from carbon contamination on the sample surface. Signals were recorded for $O(1p_{3/2})$, $S(2p_{3/2})$, $Ti(2p_{3/2})$, and $Zr(3d_{5/2})$.

The temperature dependence of the conductivity was measured between 77 K and room temperature on pressed pellets of samples with nominal composition $x = 6/8$, 5/8, 4/8, 3/8, 2/8. The choice of powders over single crystals was a trade-off between the purity of the powders and the superior conductivity measurements on single crystals which are contaminated with the halogens used as transporting agents. A two-probe, low-frequency (37 Hz) method was used. Pieces of gold foil pressed into the faces of the pellet were used to make elec-

trical contact. The ac currents were 0.1–1.0 mA and the voltage was detected by a lock-in amplifier in phase with the current source. Since it is not possible to obtain absolute resisitivities on powder samples, the ratio of the resistivity to the resistivity at 300 K is plotted to show the temperature dependences.

Results

The reaction products were platelike crystals ranging in size from 325 mesh to 2 × 2 mm for the iodine mineralized samples and about 325 mesh for the unmineralized samples. The color of the layered material varied from black to brown to gold as the titanium content was increased. The brown-to-gold transition is near the nominal composition $Zr_{0.5}Ti_{0.5}S_2$.

For samples with greater than 50 at.% titanium, an extra phase consisting of reddish needles was visible when the samples were viewed under an optical microscope. The crystals measured approximately 1 mm in length and 10 μm in width. Unfortunately, due to the small size and small quantity of this phase, it was not possible to separate these crystals from the MS_2 phase for analysis. Extra lines due to these crystals were not observed in the powder patterns of the reaction products; only lines due to MS_2 were observed.

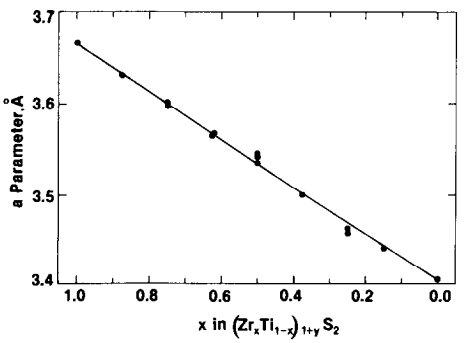

FIG. 1. Hexagonal a parameter versus composition for $(Zr_xTi_{1-x})_{1+y}S_2$ nominal composition.

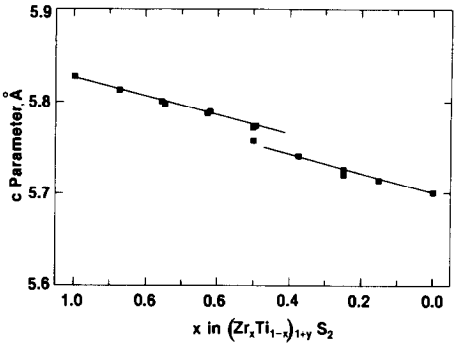

FIG. 2. Hexagonal c parameter versus composition for $(Zr_xTi_{1-x})_{1+y}S_2$ nominal composition.

The diffraction patterns of the unmineralized samples were of good quality for the compositions close to the binary phase limits and of poorer quality for intermediate compositions. The hexagonal a and c lattice parameters as determined from a least-squares fit of the data are given in Table I and plotted in Figs. 1 and 2. The lattice parameters show near Végard's law behavior with a break in the c parameter near $x = 0.5$. The c parameter obtained for $x = 0$ is that of nonstoichiometric $Ti_{1.1}S_2$ (*18*). Therefore, the break in the c parameter near $x = 0.5$ is associated with a change in stoichiometry such that the layered phases have the composition $(Zr_xTi_{1-x})_{1+y}S_2$ with $y > 0$. The red needles are produced for mass balance and by their color and shape we suggest that these are the chalcogen-rich phase MS_3.

The XPS experiments gave several interesting results. First it was noted that charging was observed for the ZrS_2 sample but not for $Zr_{0.5}Ti_{0.5}S_2$ or TiS_2, indicating that the conductivity of the latter two materials is higher than that of ZrS_2. Table II shows the binding energies recorded for the three samples. The sulfur energies are similar for $Zr_{0.5}Ti_{0.5}S_2$ and TiS_2 but different for ZrS_2, suggesting that the electronic structure of the sulfur atoms is different in the latter compound. Likewise, the zirconium energy for $Zr_{0.5}Ti_{0.5}S_2$ is also different from the zir-

TABLE II
XPS BINDING ENERGIES

Compound	S($2p_{3/2}$)	Zr($3d_{5/2}$)	Ti($2p_{3/2}$)
ZrS_2	162.68	182.79	—
$Zr_{0\sim5}Ti_{0\sim5}S_2$	161.45	181.29	456.83
TiS_2	161.56	—	456.92

conium energy in ZrS_2. Taken together with the X-ray diffraction results, these data suggest that a change in the electronic structure of these materials occurs near $x \sim 0.5$.

Figure 3 shows the XPS signal as a function of the binding energy of the Ti($2p_{3/2}$) level for the sample of nominal composition TiS_2. A notable feature is the shoulder on the main peak. The origins of this feature are unclear but three possibilities exist: (a) the shoulder is due to the TiS_3 impurity phase, (b) the shoulder is due to TiO_2 impurities, or (c) these are shake-up (relaxation) features. The first possibility can be ruled out since the peak height of the shoulder suggests that large quantities of TiS_3 are present; this is not consistent with the phase analysis. The second possibility can be ruled out also since the oxygen peaks are very small; this suggests that there is not enough oxygen on the surface to create large quantities of TiO_2 to produce the large shoulder on the Ti peak. Since this satellite also appears on the Ti($2p_{3/2}$) level in the $Zr_{0.5}Ti_{0.5}S_2$ sample which contains no oxygen peaks and no MS_3 phase, the shoulder is most likely a shake-up feature.

A plot of the log of the resistance normalized to the resistance at 293 K versus the reciprocal of the absolute temperature is shown in Fig. 4. A change in the sign of the slope occurs between the nominal compositions with $x = 0.500$ and $x = 0.375$, indicating that a metal–insulator transition occurs as a function of composition in this range. All these materials have resistivities between 1 and 100 ohm-cm. The energy of activation for conduction for samples with $0.75 > x > 0.50$ is in the range 0.01 to 0.10 eV.

Discussion

The XPS and conductivity data for the compounds $(Zr_xTi_{1-x})_{1+y}S_2$ reveal a metal–insulator transition as a function of composition in the range $0.375 < x < 0.500$. This transition is accompanied by a change in metal-to-sulfur stoichiometry, with $y \sim 0$ for $x > 0.5$, and $y > 0$ for $x < 0.5$. The change in stoichiometry is evident from a break in the c parameter versus composition at $x = 0.5$ as well as from the appearance of MS_3 needles in the reaction tubes with nominal composition $x < 0.5$.

While the a parameter changes smoothly with composition, a contraction in the c parameter is observed for $x < 0.5$. A similar anomaly in the c parameter has been observed for the metallic phases of the mixed layered systems $HfSe_{2-x}Te_x$ (*4*) and $Ti_{1+x}S_2$ (*18*) as a function of x. In the case of $(Zr_xTi_{1-x})_{1+y}S_2$, the layered phase becomes nonstoichiometric $M_{1+y}S_2$ for $x < 0.5$, and MS_3 is produced for mass balance. In the layered phases with large titanium content,

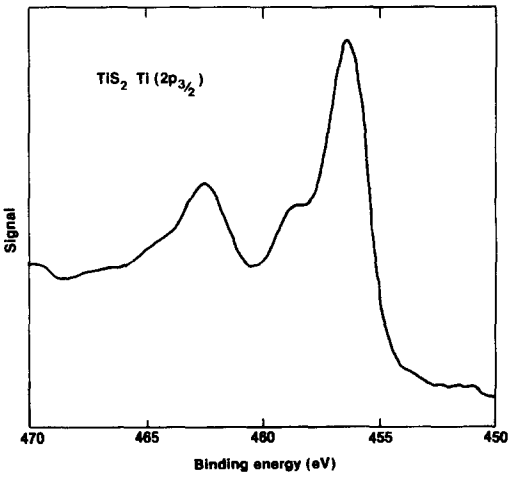

FIG. 3. XPS signal versus binding energy for Ti($2p_{3/2}$) orbital in TiS_2 nominal composition.

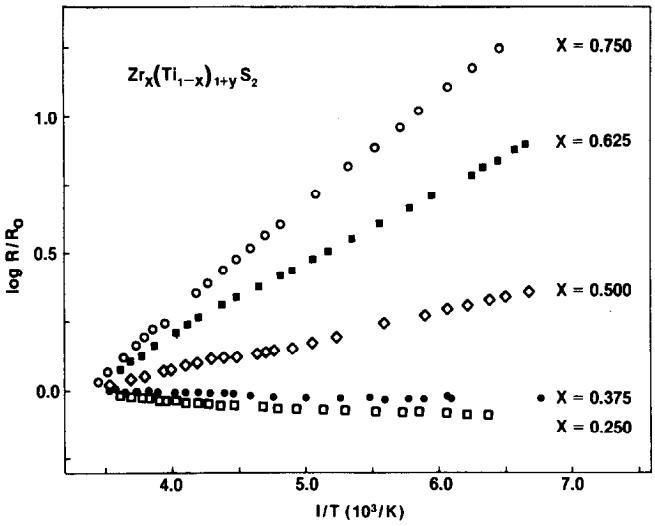

FIG. 4. Log of the ratio of resistance to room temperature resistance versus reciprocal temperature for several compositions of $(Zr_xTi_{1-x})_{1+y}S_2$ nominal composition.

the excess metal is incorporated interstitially between the layers. Since Ti^{4+} (r = 0.60 Å) is smaller than the octahedral hole in TiS_2 (r = 0.72 Å), the thickness of the van der Waals gap is reduced and the c parameter decreases for electrostatic reasons; i.e., the layers are negatively charged while the interstitial Ti is positively charged. The line drawn through the c parameter data for $x < 0.5$ extrapolates as x goes to zero to a value which is the same as that for $Ti_{1.1}S_2$ (*18*). Therefore, for the metallic phases ($x < 0.5$), y ranges from 0 to 0.1.

The XPS results show that while the titanium energy levels are the same for the compounds with $x = 0.5$ and $x = 0.0$, the zirconium levels are different for the compounds with $x = 0.5$ and $x = 1.0$. The shift in the zirconium energy levels can be attributed to a change in bonding, for example, a change from the position for the Fermi level in insulating ZrS_2 to a position in the conduction band of the conducting phase of nominal composition $Zr_{0.5}Ti_{0.5}S_2$. Similar behavior is observed for the sulfur binding energies which are the same for the two metallic compositions but higher for ZrS_2.

This study of the metal–insulator transition in the IVB layered dichalcogenides shows that the defect structure plays an important role in determining the electronic properties. The semiconducting IVB compounds are stoichiometric, while the metallic compounds are nonstoichiometric. One way to understand this behavior is to use the suggestion of Lucovsky *et al.* (*11*) that the nature of the bonding in the IVB compounds is determined by the ionic radius ratio of the cation-to-anion, r^+/r^-. When this ratio is reduced below 0.33, either a change occurs in coordination from six to four or the character of the bonding changes. In this case the phase changes its bonding from covalent to metallic while remaining six coordinate.

Since r^+/r^- is 0.33 for TiS_2, a change in bonding is predicted for compositions near $x = 0$. Stoichiometric TiS_2 is expected to have a band gap energy close to zero (*8*). Therefore, if $y = 0$ for the $(Zr_xTi_{1-x})_{1+y}S_2$ phases, as x increases the band gap energy will increase linearly and materials with x close to zero will be semiconductors. Since both arguments predict a metal–insulator transition at a value of x much smaller than

that observed, neither is valid for this system.

The phase and structural analyses clearly show that the metal–insulator transition is associated with a change in stoichiometry. The relationship between nonstoichiometry and metallic behavior is a general feature of the IVB dichalcogenides and their solid solutions. While the cause and effect relationship between the electronic properties and the nonstoichiometry is difficult to assess, the mutual dependence is clear.

Acknowledgments

The authors thank Dr. Robert Thorn for the XPS measurements and Dr. Everett Rauh for aid in making the conductivity measurements.

References

1. J. A. WILSON AND A. D. YOFFEE, *Adv. Phys.* **18,** 193 (1969).
2. See references *in* "Structural Chemistry of Layer-Type Phases" F. Lévy, Ed.), Reidel, Dordrecht (1976).
3. D. T. HODUL AND M. J. SIENKO, *Physica B & C (Amsterdam)* **99,** 215 (1980).
4. D. T. HODUL AND A. M. STACY, *J. Solid State Chem.* **54,** 438 (1984).
5. D. T. HODUL AND M. J. SIENKO, *Inorg. Chem.* **20,** 3655 (1981).
6. D. T. HODUL AND A. M. STACY, submitted for publication.
7. C. A. KUKKONEN, W. J. KAISER, E. M. LOGOTHETIS, B. J. BLUMENSTOCK, P. A. SCHROEDER, S. P. FAILE, R. COLELLA, AND J. GAMBOLD, *Phys. Rev. B* **24,** 1691 (1981).
8. A. ZUNGER AND A. J. FREEMAN, *Phys. Rev. B* **16,** 906 (1977).
9. C. UMRIGAR, D. E. ELLIS, D. WANG, H. KRAKAVER, AND M. PASTERNAK, *Phys. Rev. B: Condens. Matter* **26,** 4935 (1982).
10. J. VON BOEHM AND H. M. ISOMÄKI, *J. Phys. C* **15,** L733 (1982).
11. G. LUCOVSKY, R. M. WHITE, J. A. BENDA, AND J. F. REVELLI, *Phys. Rev. B: Condens. Matter* **7,** 3859 (1973).
12. R. NITSCHE, *Fortschr. Mineral.* **44,** 231 (1967).
13. I. TAGUCHI, *Solid State Commun.* **32,** 679 (1979).
14. F. MEHRAN, T. D. SCHULTZ, M. W. SCHAFER, AND W. J. FITZPATRICT, *Phys. Rev. Lett.* **33,** 1085 (1974).
15. I. TAGUCHI, *J. Phys. C* **14,** 3221 (1981).
16. H. P. KLUG AND L. E. ALEXANDER, "X-Ray Diffraction Procedures," Wiley, New York (1954).
17. M. U. COHEN, *Rev. Sci. Instrum.* **6,** 68 (1935); **7,** 155 (1936).
18. A. H. THOMPSON, F. R. GAMBLE, AND C. R. SYMON, *Mater. Res. Bull.* **10,** 915 (1975).